© 2002

Determination of Total Acid in Palygorskite Chemically Modified by N-Butylamine Thermodesorption

Juan A.C. Ruiz[a]*, Dulce M.A. Melo[a], José R. Souza[b], Leopoldo O. Alcazar[b]

[a]*Post-Grad. Prog. in Chemistry*
[b]*Post-Grad. Prog. in Chemical Engineering Federal*
University of Rio Grande do Norte, University Campus Lagoa Nova
59078-970 Natal - RN, Brazil

The acid properties of palygorskite clay (R1) were studied using n-butylamine as probe molecule. A comparison was made of these properties in palygorskite clay (R1), in an acidified palygorskite (R2) and in acid palygorskite loaded with 2% of lanthanum (R3). The total acid properties were determined by FTIR (Fourier Transform Infrared) and TG-DTA (thermogravimetry). The acidity increased as follows: R3 > R2 > R1. The acid strength sites were classified as physisorbed, weak, medium and strong. The acid treatment did not change the site distribution, apparently only removing channel impurities. The introduction of lanthanum created many more acid sites and increased the specific area. Both weak and strong sites, which increased significantly, were considered new active acid sites produced by the lanthanum.

Keywords: *palygorskite, lanthanum, thermodesorption, acid catalyst*

1. Introduction

Clay, a naturally occurring material composed primarily of fine-grained minerals, is usually plastic when its water content is appropriate, hardening when dried or fired. Clays can contain aluminum, magnesium, and iron hydrate silicates in their chemical composition[1].

Clays have been increasingly utilized as catalysts and catalyst supports owing to their excellent properties, such as high adsorption capacity, surface area, and easy ion exchange[2]. Due to the large number of specific cation exchanges, these materials can be used as catalysts in many industrial reactions. These exchanges can create a variety of specific reaction sites on the surface[3].

When subjected to proper acid treatment, some clays undergo changes in their surface area and in the number of active acid sites. These changes are caused by the removal of impurities and by the exchange of protons and structural metal cations[4]. After this treatment, therefore, a material whose superficial topology has been modified can be used in different applications, i.e., as an adsorbent[5], a color remover[6], a catalyst or a catalyst support[7].

A relevant characteristic of the hormite clay group is its hollow fiber structure. This group's structural models differ significantly from the layered models because of the fiber-type arrangement of its crystals, with ribbon-like structural units rather than layers. One of the clays of this group is palygorskite, which is formed naturally by chemical precipitation in closed lakes or seas, where acid volcanic ash and/or soluble salts are often present[8]. Palygorskites are hydrated magnesium silicates with partial isomorphic substitutions of magnesium by aluminum and/or iron. A two-layer clay consisting of tetrahedral SiO_4 and $Al(OH)_3$ with an octahedral $Mg(OH)_2$ layer between them can be classified as a 2:1 type. Bradley (1940) was the first to propose a structure, introducing the theoretical formula $[Si_8Mg_5O_{20}(OH)_2](H_2O)_4.4H_2O$[9]. This clay has a fibrous texture with an internal structure of microchannels and different bonded water molecules representing almost 20% of the structure's total weight[10].

Lanthanides, in turn, play an important role in certain technological developments and are key constituents in technological applications such as catalyst synthesis, ceramics, laser, etc.

Lanthanum is a lanthanide that has been extensively studied as a catalytic material. It can be used in numerous reac-

*e-mail: jachr7@yahoo.com

tions, among them nitrogen oxide reduction of combustion exhaust gas, methanol synthesis as a promoter of noble metals (Pt, Pd), oxidative coupling of methane reactions, etc. A material having the structural properties of palygorskite and the catalytic benefits of lanthanum is therefore highly desirable.

The introduction of lanthanum into the palygorskite structure can modify the latter's surface characteristics, changing the material's catalytic properties. An easily determined surface property is total surface acidity (TSA). Thus, the modification of palygorskite by the introduction of lanthanum creates new active sites, increasing the clay's catalytic properties, such as its activity, selectivity and thermal stability. An example of the influence of lanthanide is zeolite Y modified by rare earth (RE) ion exchange, in which the new catalytic properties result from the formation of a hydroxilic species inside the zeolitic channel, followed by cation-induced thermal hydrolysis after calcination to produce $RE(H_2O)_n^{3+}$ [11].

Determining a material's TSA provides valuable information about the nature of its acid sites, their acid strength and the site distribution along the catalyst. This information can also provide clues about the possible applications of the material and shed light upon its catalytic behavior.

In this paper, we report on a study of surface acid properties, using thermodesorption of n-butylamine as the probe molecule in three materials: pure palygorskite (R1), acidified palygorskite (R2) and acid-palygorskite containing 2% of lanthanum (R3). Two main characterization methods were employed in this study, i.e., Fourier transform infrared spectroscopy (FTIR) and thermogravimetry (TG, DTA).

2. Experimental

The palygorskite used in this study was collected in the state of Piauí, on Brazil's northeastern coast. Although it was used in its natural state, it underwent several modifications resulting from the laboratory manipulations described below.

A. Acidification and impregnation procedure

The palygorskyte acidification procedure consisted of adding a hydrochloric acid solution 6N to the untreated solid (R1) in a stirred reactor with water reflux. The slurry concentration was 15% in weight of the total solids. The procedure was conducted at a temperature of 353 K with an initial pH of 0.88, under 5 hours of continuous agitation (1800 rpm), after which the material was dried and sieved. The fraction between 80 – 100 mesh was separated for further use (R2).

Part of the acidified palygorskite was soaked in a solution of $La(NO_3)_3$. The lanthanum ion, La^{+3}, was introduced into the R2 by ion exchange. Impregnation was carried out at 353 K for 48 h under continuos stirring, in a pH range of 4 to 5. After it was dried, the material was loaded with 2% (w/w) lanthanum and is referred to hereinafter as R3.

B. N-butylamine adsorption / desorption

Samples of approximately 50 mg of the R1, R2 and R3 materials were placed in a fixed bed reactor. Each sample was initially activated by passing through it a N_2 flux of 30 ml min⁻¹ at 673 K for 1 hour. A nitrogen stream saturated with n-butylamine at 373 K was then made to flow through the bed for 1 hour. Finally, the bed was flushed with pure N_2 in order to remove the physisorbed n-butylamine. This procedure was repeated with each material and the products were dubbed R1A, R2A and R3A, respectively.

C. Characterization methods

All the samples, R1, R2, R3, R1A, R2A and R3A, were characterized by infrared spectroscopy, thermogravimetry, specific surface area methods and X-ray diffraction. The infrared spectroscopy of the samples was performed using a BOMEN FTIR spectrometer over a KBr disk in a wave number range of 1700 – 1300 cm⁻¹. For the thermogravimetric experiments, samples of aproximately 2.5 mg were loaded into a Perkim Elmer TGA-7 thermobalance. The tests were performed under a dynamic N_2 atmosphere of 50 ml min⁻¹ flux, in a temperature range of 300 to 1173 K and a heating rate of 10 K min⁻¹. The materials' surface areas were determined by the BET method, using a Flowsorb 2300 Micromeritics device with liquid nitrogen at 77 K. The X-ray spectra were obtained with a Shimadzu XD3-A X-Ray Diffractometer (30/20 kV/ Ma) in the 2θ range of 1.5 to 40 degrees, at a scanning rate of 2 degrees min⁻¹ and CuKα radiation.

Table 1. Characteristic X-Ray peaks for different clay minerals identified in the samples.

Clay	2θ °	I/Io	h	k	l	Ref.
Palygorskite	8.50	100	1	1	0	(12)
	13.92	20	2	0	0	
	28.05	18	4	0	0	
Kaolinite	12.46	100	0	0	1	(13)
	25.01	100	0	0	2	
Illite	17.73	30	0	0	2	(14)
	20.04	100	1	1	0	
	36.75	16	1	3	1	
Quartz	20.86	16	1	0	0	(14)
	26.64	100	1	0	1	

3. Results and Discussion

Figure 1 displays the X-Ray diffractograms of the R1, R2 and R3 samples. Table 1 shows several clay materials with their respective characteristic peaks. Figure 1a depicts the diffractogram of the untreated material. The peaks at 2θ 8.5, 13.92 and 28.05° confirm the presence of palygorskite. Other peaks were also identified and correspond to the mineral clays listed in Table 1. It was concluded that most of the starting material was indeed palygorskite, although it contained some impurities.
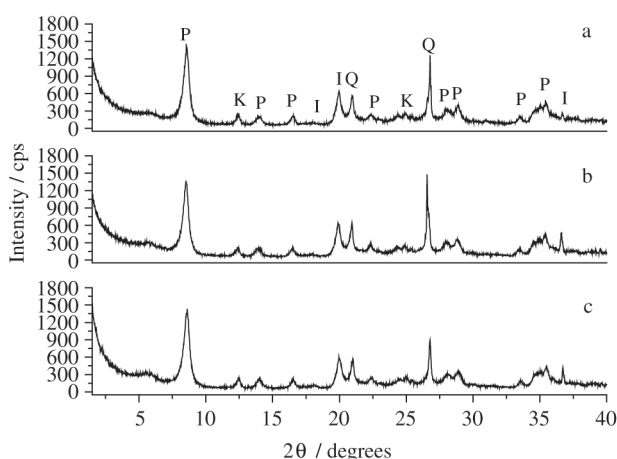
Figure 1b shows a diffractogram of the acidified clay (R2). Basically, this diffractogram does not differ from that of the R1 material, although a careful analysis of the peaks at 2θ = 26.78° and 36.60° reveals an increase in their intensities, suggesting minor structural changes that did not, however, affect the clay's basic mineral structure.

The lanthanum-containing sample also showed no significant changes (Fig. 1c). Hence, it can be assumed that the introduction of lanthanum into the octahedral regions did not change the material's geometry. Although the intensity of the peak at $2\theta = 26.78°$ diminished significantly, this was attributed to structural recovery.

An interesting fact revealed by the diffractograms was that the material's structural array remained unchanged, even with drastic acid treatment.

The IR spectra of samples R1, R2 and R3 are shown in Fig. 2a. No acid sites were found in the range of 1700 to 1300 cm^{-1}. Instead, the R1A, R2A and R3A spectra depicted in Fig. 2b reveal the presence of peaks typical of Lewis and Brönsted acid sites, which can act as catalytic acid sites. The samples' spectra (R1A, R2A and R3A) display peaks in the region of 1450 – 1470 cm^{-1} due to Lewis-type acid sites. Lewis-Brönsted sites are evidenced between 1500 – 1530 cm^{-1}, while Brönsted sites are located in the range of 1530 – 1570 cm^{-1}. These results are very similar to those reported by Parry[15] in his infrared study of pyridine adsorbed on acidic solids. As reported by Melo *et al.*[7], a better resolution of the Lewis-type acid site is visible when terbium is supported on palygorskite. This may indicate the improved interchange of the terbium atom due to its smaller atomic radius compared to that of lanthanum.

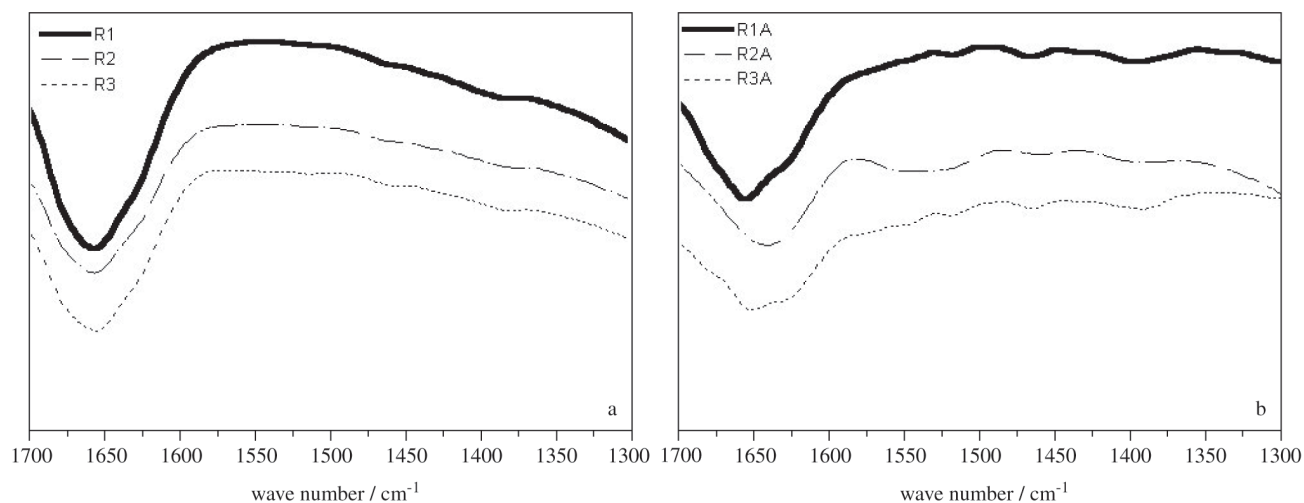Infrared spectroscopy and thermogravimetry are tech-

Figure 1. X Ray Diffractograms of R1 (a), R2 (b) and R3 (c). P: Palygorskite, I: Illite, K: Kaolinite, Q: Quartz

Figure 2. IR spectra of (a) Unadsorbed samples: R1, R2, R3; (b) N-butylamine adsorbed samples: R1A, R2A, R3A, in N_2 saturated stream at 30 ml min^{-1}, T=373 K.
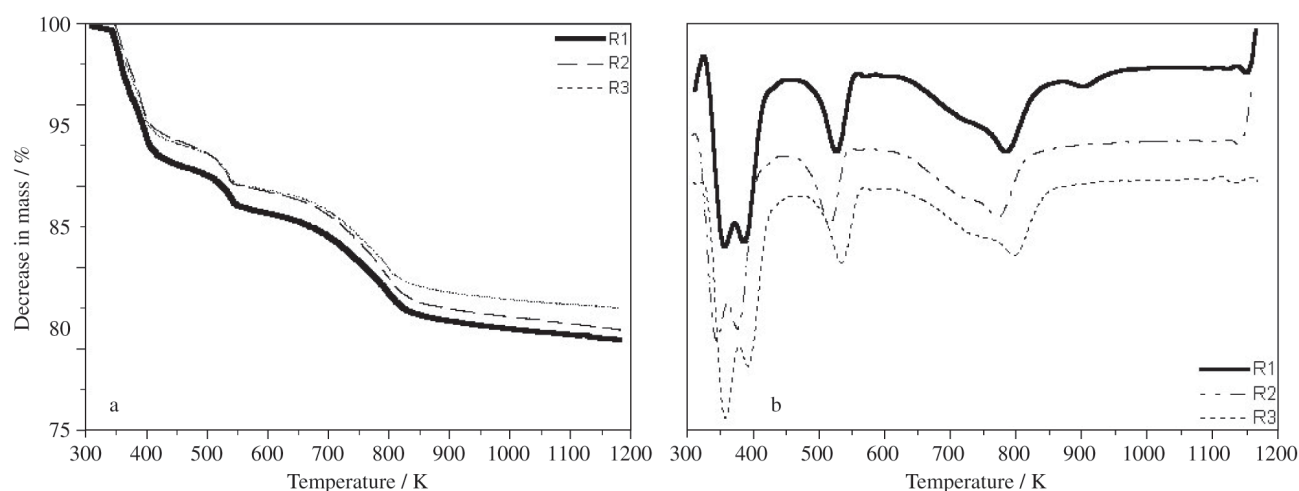
Figure 3. (a) Thermogravimetric curves of R1, R2, R3; (b) Mass derivatives of R1, R2, R3. N_2 50 ml/min flux, 10 k min^{-1} heating rate.
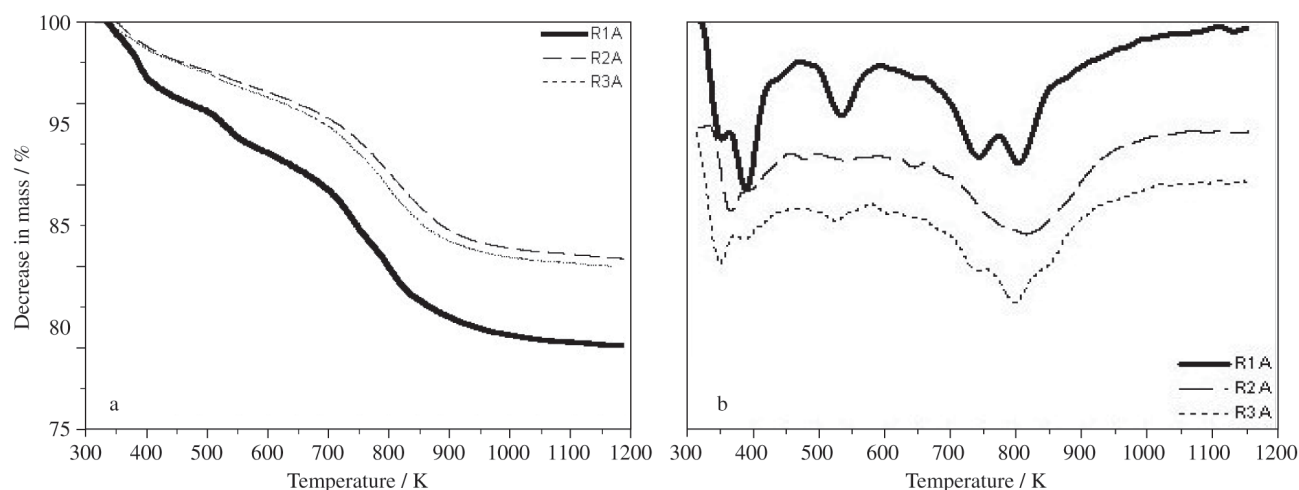

Figure 4. (a) Thermogravimetric curves of R1A, R2A, R3A; (b) Mass derivatives of R1A, R2A, R3.

niques that provide important information about the type of and total acidity of the material.

In our thermogravimetric analysis, the identification of the mass loss steps was based on the work of Barrios *et al.*[10], who elucidated the mass loss characteristics of acidified and non-acidified palygorskyte with varying concentrations of hydrochloric acid.

The thermograms and the derivatives of samples R1, R2 and R3 are presented in Figs. 3a and 3b, respectively. Three types of water loss were identified. The first loss was the water adsorbed at 300 – 383 K, followed by the zeolitic and channel deposited water loss occurring between 383 and 483 K and, finally, the bonded water loss (from the octahedral metal – water bond). This was a two-step loss, the first step ranging from 483 to 603 K and the second from 603 to

Table 2. Adsorption site distribution in R1, R2 and R3.

Adsorption site (mmol.g^{-1})	Desorption range (ΔT) K	Material		
		R1	R2	R3
Physical adsorption	300-383	0.116	0.166	0.152
Weak chemisorption	383-483	0.156	0.231	0.571
Medium chemisorption	483-603	0.149	0.226	0.386
Strong chemisorption	603-993	0.169	0.269	0.617

873 K. As can be seen, all the samples displayed similar behavior except the first water loss in sample R1.

The thermograms and first derivatives of the adsorbed samples are shown in Figs. 4a and 4b, respectively. An analysis of the thermograms reveals four temperature ranges for

n-butylamine desorption: the physically adsorbed n-butylamine in the 300 to 383 K range, the weakly bonded sites from 383 to 483 K, the medium bonded sites from 483 to 603 K, and lastly, the strongly bonded sites in the 603 to 993 K range.

The acidity calculations were based on a 1:1 adsorption stoichiometry (1 n-butylamine molecule to 1 adsorption site). The mass of adsorbed n-butylamine per initial mass of catalyst was calculated based on the difference found between the adsorbed and unadsorbed thermograms of each material. Thus, the mass of the probe molecule adsorbed onto the different sites per gram of support was obtained within different temperature ranges. The specific total acidity (STA) was the sum of the mass adsorption in all the sites per gram of support, while the total acidity density (TAD) was the STA divided by the BET surface area. Because the adsorbed n-butylamine was preheated to 673 K, the mass loss in the 300 to 673 K range was considered a loss of n-butylamine molecules only.

Table 2 presents the site distribution for the three materials according to their adsorption strength (temperature desorption range).

The sum of the sites of materials R1, R2 and R3 yields the total acidity sites, as shown in Table 3. The 2% lantha-

num-impregnated palygorskite showed about three times more sites than the non-acidified material and almost double the number of sites of the acidified sample. Thus, the acid treatment with 6 N HCl favored the increase of acid sites in the material. This treatment also aided lanthanum deposition, further increasing the number of acid sites. The surface area and surface density sites are also given in Table 3.

As Fig. 5 reveals, the greater number of acid sites in the acidified material are distributed equally among all the types of acid sites. The lanthanum-palygorskite material showed a slightly greater increase of Lewis (weak) sites than of other sites.

4. Conclusions

The acid treatment applied in this study satisfactorily increased the acidity of palygorskite and also favored lanthanum impregnation of the material.

The three materials, R1, R2 and R3, showed Lewis and Brönsted acid sites, which were classified as having weak, medium and strong acid strength. These sites were identified by the thermodesorption of n-butylamine adsorbed in the material.

The lanthanum-modified palygorskite displayed the greatest surface area and largest number of acid sites. Although this material developed both Lewis and Brönsted acid sites, a greater number of Lewis sites were evidenced by the IR spectra.

Table 3. Material properties.

Property	Material		
	R1	R2	R3
Surface Area ($m^2 g^{-1}$)	168	150	178
Specific Total Acidity ($mmol\ g^{-1}$)	0.476	0.767	1.574
Total Acidity Density ($mmol\ cm^{-2}$)	28.33	51.13	88.42

Figure 5. Cumulative acid site distribution in samples R1, R2, R3.

References

1. Guggenheim, S.; Martin, R.T. *Clay and clay Minerals,* v. 43, n. 2, p. 255-256, 1995.
2. Gomes, C.F. *Argilas: O que são e para que servem.* Cap. 2 e 13, Lisboa: Fundação Calouste Gulbenkian, 1986.3. Coelho, A. C., Santos, P. S. *Revista Brasileira de Química*, v. 11, p. 26-37, 1988.
4. Myriam, H. M.; Suarez, M.; Martin-Pozas, J.M. *Clays and Clay Minerals*, v. 46, p. 225-231, 1998.
5. Campelo, J.M.; García, A.; Luna, D.; Marinas, J.M. *Clay Miner.*, v. 25, p. 207-215, 1987.
6. Souza, J.R.; Melo, M.A.F.; Melo, D.M.A. *Clarificação de efluentes da indústria têxtil utilizando vermiculita ativada como agente adsorvente*, Anais do 2º COBEQ-IC, Uberlândia, MG, 1997.
7. Melo, D.M.A.; Ruiz, J.A.C.; Melo, M.A.F.; Sobrinho, E.V.; Schmall, M. *Microporous and Mesoporous Materials*, v. 38, p. 345-349, 2000.
8. Baraúna, O.S.; Araújo, A.P.R.; Santos, H.S.; Santos, P.S. *Cerâmica*, v. 32, p. 339-350, 1986.
9. Zandonadi, A.R.; Skitnevski, I. *Cerâmica*, v. 32, p. 333-338, 1986.

10. Barrios, M.S.; Gonzales, L.V.F.; Rodriguez, M.A.V.; Martin-Pozas. J.M. *Applied Clay Science*, v. 10, p. 247-258, 1995.

11. Sousa-Aguiar, E.F.; Camorim, V.L.D.; Zotin, F.M.Z.; Santos, R.L.C. *Microporous and Mesoporous Materials*, v. 25, p. 25-34, 1998.

12. Christ, C.L.; Hathaway J.L.; Hostetle P.B.; Shepard A.O.

13. Brindley, G. Penn State Univ., University Park, USA, ICDD grandt-in-Aid, 1977.

14. Kern, A.; Eysel, W. Mineralogisch-Petrograph. Inst., Univ. Heidelberg, Germanny, ICDD Grant-in-Aid, 1993.

American Mineralogist, v. 54, p. 198-&, 1969.

15. Parry E.P. *Journal of Catalysis*, v. 2, p. 371-379, 1963.